Topics in Catalysis Vol. 33, Nos. 1–4, April 2005 (© 2005)
DOI: 10.1007/s11244-005-2514-4

Support and dispersion effects on activity of platinum catalysts during wet oxidation of organic wastes

Z.P.G. Masende[a,b], B.F.M. Kuster[a,*], K.J. Ptasinski[a], F.J.J.G. Janssen[a], J.H.Y. Katima[b], and J.C. Schouten[a]

[a]*Laboratory of Chemical Reactor Engineering, Department of Chemical Engineering and Chemistry, Eindhoven University of Technology, P.O. Box 513, 5600 MB Eindhoven, The Netherlands*
[b]*Department of Chemical & Process Engineering, Faculty of Mechanical and Chemical Engineering, University of Dar es Salaam, P.O. Box 35131, Dar es Salaam, Tanzania*

Catalytic activity of platinum catalysts such as Pt/graphite, Pt/TiO_2, Pt/Al_2O_3, and Pt/active carbon was studied using a slurry phase CSTR. Three model reactions, namely, phenol, maleic acid, and malonic acid oxidation were investigated in the temperature range from 120 to 170 °C and at a total reactor pressure of 1.7 MPa. Platinum on graphite was found to be most suitable for aqueous phase oxidation of phenol, maleic acid, and malonic acid. Complete conversion for both phenol oxidation as well as maleic acid oxidation to CO_2 was observed with Pt/graphite at stoichiometric oxygen excess close to 0% and at 150 °C. Deactivation due to over-oxidation is gradual for Pt/graphite with a metal dispersion of 5.3% as compared to Pt/TiO_2, Pt/Al_2O_3 and Pt/AC, which have metal dispersions of 15.3%, 19.5% and 19.0%, respectively. It was further found that in the presence of Pt/graphite catalyst and oxygen, malonic acid reaction proceeds via non-catalysed decarboxylation, and catalytic decarboxylation to CO_2 and acetic acid, and catalytic oxidation to CO_2 and H_2O. Acetic acid was found to be difficult to oxidise at temperatures below 200 °C.

KEY WORDS: platinum catalysts; catalytic supports; wastewater treatment; stoichiometric oxygen excess; platinum metal dispersion

Nomenclature

AC	active carbon
	concentration of the compound i [mol/m^3]
CWO	catalytic wet oxidation
	molar flow rate of compound i [mol/s]
	volumetric flow rate [m^3/s]
F_V^L	volumetric flow rate of liquid [m^3/s]
n_c	number of carbon atoms in a compound [–]
P	pressure [Pa]
Pt	platinum
$R_{w,i}$	specific disappearance rate of compound i [mol/s.kg]
SCWO	supercritical water oxidation
$S_{\rightarrow i}$	selectivity to compound i [%]
S.E.	stoichiometric oxygen excess to model compound [%]
T	temperature [K]
V_L	volume of the liquid in the reactor [m^3]
W	total mass of dry catalyst in the reactor [kg]
WAO	wet air oxidation
	conversion of compound i [%]

Superscripts

l	liquid
L	liquid

Subscripts

ads	adsorbed
C	carbon atoms
cat	catalyst
i/j	organic compound
in	inlet to reactor
Ph	phenol
w	weight

*To whom correspondence should be addressed.
E-mail: b.f.m.kuster@tue.nl

1. Introduction

Cleaning of hazardous and toxic organic wastes in water before the final disposal has acquired great importance all over the world in order to protect the human health, aquatic life, and the whole environment. The treatment of industrial wastewater, which contains organic wastes, by biological processes, is often unsuitable due to their inherent toxicity to micro-organisms. The use of traditional non-catalytic chemical processes or incineration may be too costly and energy intensive. Conventional wet air oxidation (WAO) processes usually require higher pressures (0.5–20 MPa) and temperatures (423–598 K), which result in a high capital investment and a high energy consumption for operation. The application of homogeneous and heterogeneous catalysts can improve the oxidation efficiency of organic wastes in water and reaction temperatures can be reduced [1,2]. Homogenous catalysts are reported to be more effective in increasing the rate of oxidation, but heterogeneous catalysts are preferred because the catalyst is present as a separate phase and therefore more likely easy to separate.

Catalytic wet oxidation (CWO) using solid catalysts, involves the following steps: diffusion of the reactants to

1022-5528/05/0400–0087/0 © 2005 Springer Science+Business Media, Inc.

the catalytic or support surface, adsorption of the reactants onto the surface, reaction on the surface, desorption of products off the surface, and diffusion of products from the surface. Because of these steps, heterogeneous processes are usually more complicated to control. Since the catalyst surface plays an important role in adsorption and desorption, appropriate selection of both the active part and the support of the catalyst therefore can have a remarkable effect on the reaction rate.

The advantages and disadvantages of supported and unsupported non-noble (transition) metal oxides and noble metals for catalytic wet oxidation of organic pollutants have been well reviewed [1,3,4]. Supported noble metal catalysts, like platinum catalysts, are generally less vulnerable to deactivation by leaching of the active metal and show higher overall activities for the oxidation of pollutants [3]. However, platinum catalysts may suffer rapid loss of catalyst activity, which is due to either poisoning by surface impurities, or deactivation due to too high oxygen coverage (over-oxidation). It was previously found that the deactivation of a Pt/graphite catalyst could be avoided by operating the reactor within a practical operation window, whereby moderate oxygen coverage of the platinum surface could be maintained [5]. The role and influence of the catalyst support on the reaction mechanism and on the stability of the platinum catalyst were not investigated.

According to Matatov-Meytal and Sheintuch [1], the support serves three important functions in the catalytic system, namely, to increase the surface area of the catalytic material; to decrease sintering and to improve hydrophobicity and thermal stability and chemical stability of the catalytic material; and to govern the lifetime of the catalyst. Supports may also improve the catalytic activity by acting as a co-catalyst. Reducing the crystallite size of the active metal, or increasing the dispersion, increases the active surface area. However, very small active metal particles are vulnerable for oxygen poisoning due to the high enthalpies of oxygen adsorption on small metal particles particularly under 2 nm [6]. Another possibility to increase activity is to increase the particle porosity. Supporting the noble metal catalyst on a metal oxide surface has been suggested to improve the activity and stability of the catalyst [7]. However, a hot and acidic medium promotes solubility of some transition metal oxides and therefore causes deactivation of the catalyst by leaching of the metal or metal oxides [1]. Beziat *et al.* [6] reported a high stability of titania supported ruthenium catalyst, when used in acidic and oxidizing medium for oxidation of aqueous solutions of carboxylic acids. While noble metal catalysts supported on activated carbon are more resistant to acidic leaching than transition metal oxides [6,8], activated carbon is likely to burn off at higher temperatures [9].

The support may influence the surface properties of the platinum particles due to platinum-support interaction. According to Gallezot *et al.* [10], the different interaction with the graphite support of platinum particles located at the edges of basal planes and particles on top of basal planes is due to electron transfer from the graphite to the platinum particles at the edges of basal planes, resulting in a different morphology and electronic structure. The rate of liquid phase oxidation may also be influenced by the hydrophilic character of the catalyst, which is related to the number and nature of the support surface groups. This may influence the affinity of the support for the aqueous phase or the physisorption of the organic compound on the support and thereby the internal transport of the organic compound or adsorption of the organic compound on the active platinum surface [11]. For catalytic wet oxidation, it is therefore worthwhile to understand not only the reaction conditions, but also the morphology, texture, and size of the catalyst support, and the location of the active metal.

The reactor configuration and the mode of operation may cause significant impact on performance of the platinum catalysts. Most of the kinetic studies in catalytic wet oxidation (CWO) have been carried out in batch reactors [1,2]. The advantages of batch reactors include simplicity in operation, flexibility in production and process operations, and simplicity in determination of kinetic rates [12–14]. Whereas batch reactors are helpful in measuring of intrinsic kinetics in the absence of catalyst deactivation, unfortunately, most of heterogeneous catalytic reactions using noble metal catalysts, are affected by, among others, deactivation due to over-oxidation. Due to these reasons a continuous stirred tank reactor (CSTR) is preferred for quantifying simultaneously reaction and deactivation kinetics [12].

In the present work, attention is focused on the understanding of the reaction mechanisms of platinum catalysts during oxidation of organic wastes in water. Different supports for platinum metal catalysts are evaluated. These include carbon-based, namely: Pt/graphite (G) and Pt/active carbon (AC), and Pt/Al_2O_3 and Pt/TiO_2, being metal oxide supports. The effect of the reaction conditions on the properties of the catalysts was investigated. Phenol was used as a model reaction since it is one of the most serious pollutants and is considered as worst case in WAO studies. Maleic acid was investigated because it is one of the intermediate products reported in the phenol reaction network. Malonic acid was also investigated since it is an intermediate to acetic acid [15]. The investigation was carried out in a slurry phase CSTR.

2. Experimental

The experimental work was carried out at the Laboratory of Chemical Reactor Engineering at Eindhoven University of Technology (Netherlands)

and at the Department of Chemical & Process Engineering at the University of Dar es Salaam (UDSM) in Tanzania. In both laboratories, the same type of reactor set-up was used. Whereas oxidation of phenol was performed at Eindhoven University of Technology, the experiments for maleic acid and malonic acid oxidation were carried out at University of Dar es Salaam. Whenever there are differences, e.g. materials and equipment used at the University of Dar es Salaam, it is stated in this paper.

2.1. Chemicals and catalyst

All chemicals used in this research including phenol, maleic acid, and malonic acid were pure analytical grade from Merck, and were used as received. Oxidation solutions were prepared using deionised water. Gases were of 99.99% purity (5.0 grade) from Hoekloos (Netherlands). In Tanzania, all gases (99 + %) were obtained from Tanzania Oxygen Limited (TOL). The liquid phase oxidation of organic solutions was investigated using commercially available catalysts namely, Pt/graphite (5 wt%) from Johnson Matthey, and Pt/active carbon (5 wt%), Pt/Al_2O_3 (5 wt%) and Pt/TiO_2 (5 wt%) from Engelhard. The metal content for both fresh and used catalysts, average catalyst particle diameter and the particle size distribution, and the morphological properties were determined as described below.

2.2. Catalyst characterisation techniques

The morphology of the catalyst particle was examined using a scanning electron microscope (SEM) apparatus. The samples were prepared by forming a thin layer (70 nm) of gold on a sticky carbon support with the catalyst samples on top. The gold was added to avoid charging of the catalyst samples. The topographical analyses of different catalysts were made up to a magnification of 25,000 times. The centre of the images was preserved during magnification. The signal of the secondary electrons was used for a topographical observation of the catalyst surface. The information on the particle shape and on the size of the catalyst support was obtained from the SEM micrographs. The average catalyst particle diameter and the particle size distribution were also measured with a Coulter LS 130 apparatus. Table 1 shows the results of the particle size distribution of different catalysts.

The specific surface area and metal dispersion of the platinum catalysts of different supports were analysed using the ASAP 2000 apparatus (Micromeritics Instrument Corporation). The samples for the analysis were fresh and used catalysts, which were used without any pre-treatment. The specific surface area of the catalysts was measured with a standard method of BET, which is based on the adsorption isotherm of nitrogen [16]. The porosity of catalyst support was measured by using the AutoPore IV 9500 apparatus (Micromeritics Instrument Corporation), which uses mercury as a pressure fluid. The results of BET and mercury porosity measurements are shown in table 1.

The platinum content of the catalysts was determined in duplicate by dissolving the platinum after boiling the catalysts in aqua regia (HCl/HNO_3, 3:1). This was followed by the removal of the nitric acid by adding hydrochloric acid and evaporating. For each sample, this step was done three times. On addition of a hydrochloric acid containing tin chloride solution, a stable yellow platinum tin (Sn–Pt) complex was formed by platinum ions and $SnCl_2$ in the presence of excess chlorine ions. The resulting extinction was measured by UV/VIS spectrophotometry at 403 nm [17]. Similarly, liquid samples were taken directly from the reactor to measure the loss of platinum metal by leaching during oxidation. In all samples, hydrochloric acid was added to avoid precipitation or reduction of the platinum ions prior to measurement. The platinum metal concentration in the liquid effluent was found to

Table 1
Characteristics of the supported platinum catalysts

Feature	Pt/Graphite	Pt/TiO_2	Pt/Al_2O_3	Pt/AC
Code	5R2287	42380	7080	7002
Active metal content	5% on dry basis	5% on dry basis	5% on dry basis	5% on dry basis
Type	Reduced/dry	Reduced/dry	Reduced/dry	Reduced/dry
Carrier	Graphite powder	TiO_2	Al_2O_3	Carbon
Catalyst particle size distribution[a]	<5 μm (15%)	<15 μm (10%)	<46 μm (10%)	<3.16 μm (10%)
	<10 μm (75%)	<40 μm (50%)	<74 μm (50%)	<4.71 μm (50%)
	<15 μm (95%)	<65 μm (90%)	<130 μm (90%)	<6.72 μm (75%)
	>15 μm (5%)			<10.2 μm (90%)
Total surface area (B.E.T.) [$m^2\ g^{-1}$]	15.0	70	110	100
Metal dispersion[b] [%]	5.3	15.3	19.5	19.0
Porosity[c] [%]	69.3	73.8	76.9	81.7

[a]The particle size distribution was confirmed using the Coulter LS 130 apparatus.
[b]Catalyst characterisation using ASAP 2000 series equipment.
[c]Porosity measurement using AutoPore IV 9500 equipment.

be less than 1 mg/mL[3] in all experiments whereas the maximum loss of platinum metal on the used catalyst samples was found to be less than 0.5 wt%.

2.3. Oxidation experiments

The experiments were conducted in a continuous flow stirred slurry reactor (CSTR), a 500 mL autoclave (Autoclave Engineers, Zipperclave Hastelloy) that is equipped with a gas dispersion impeller. The reactor operating conditions are given in table 2. During reaction, the reactor was kept at constant temperature within ± 0.3 K, in a wide range of temperatures, by a heating element around the reactor. The pressure in the reactor was kept constant by using a backpressure regulator. During the experiments, the flow rates of the phenol feed solution and the gas entering the reactor were kept constant. Details of the experimental set-up and reactor start-up procedures are reported elsewhere [5].

In each experiment, the progress of the reaction and the catalytic activity were monitored by measurement of the reactor effluent composition as a function of time on stream. The liquid samples were analysed by using two HPLC set-ups (Thermo Separation Products) for residual phenol and intermediate reaction products. Phenol and other aromatic compounds were analysed in a 300×4.6 ID mm Lichroma SS column, packed with a Benson type of cation-exchange resin (Ca^{++}) using a UV detector, while carboxylic acids were analysed in a 300×8 ID mm RSpak KC-811 column using a refractometer detector (Waters R401). The same HPLC columns were used at UDSM in Tanzania with HPLC set from Merck-Hitachi. The composition of the outlet gases was analysed using an on-line Gas Chromatograph (GC) (HP 5890A Series II). The GC was equipped with a 10 m Molsieve 5A wide bore (Chrompack) column, a 25 m Porapak Q wide bore (Chrompack) column, a TCD and an integrator (DataJet CH2). In addition, the oxygen concentration in the outgoing gas stream was determined by using an O_2 sensor (Orbisphere Laboratories, Switzerland). Nitrogen gas was used as a standard, while helium was used as carrier gas. In Tanzania, the composition of the effluent gases (mainly O_2, CO_2 and N_2) was determined using an online gas analyser (Servomex, Xentra 4200) where nitrogen was an inert gas during reaction.

The experimental results were evaluated in terms of the disappearance rate of the respective compound, i, using the equation

$$R_{w,i} = (F_V^l/W)(C_{i,in} - C_i) - (V_L/W)(dC_i/dt) \quad (1)$$

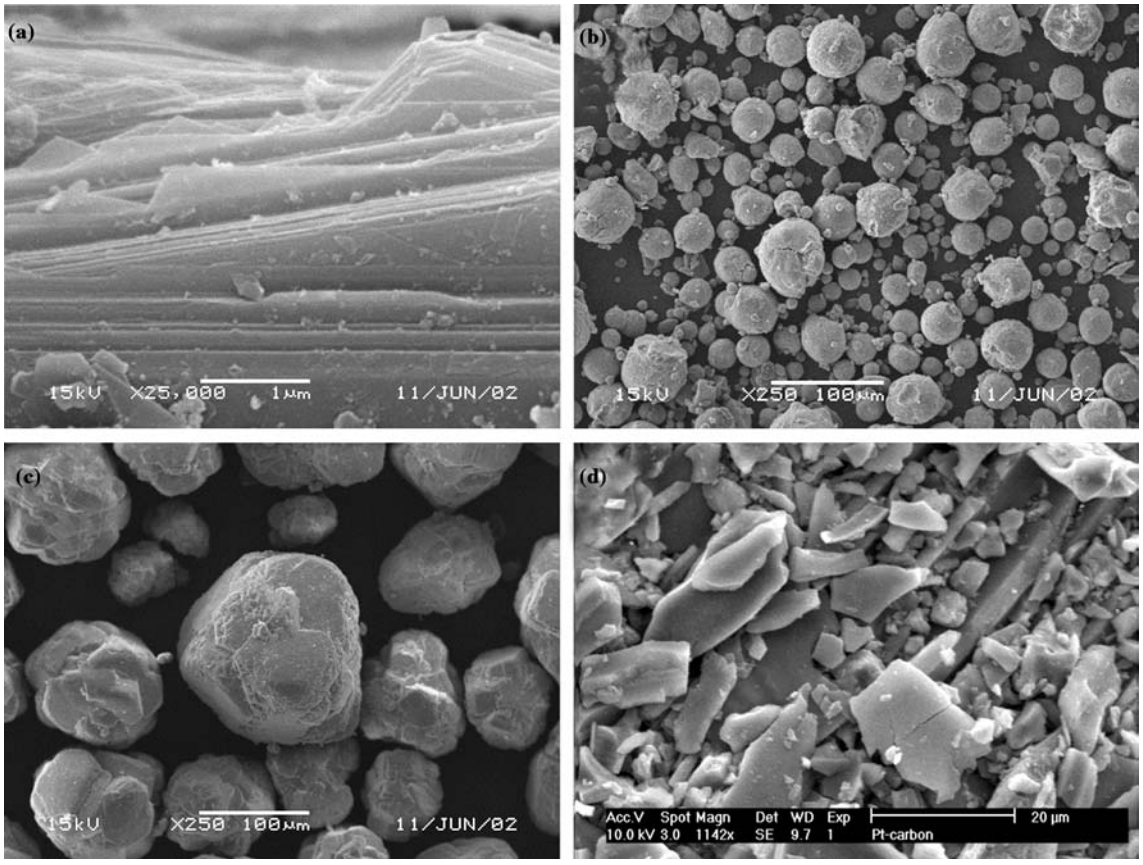


Figure 1. SEM micrographs of platinum catalysts at different magnifications: (a) Pt/graphite at X25,000, (b) Pt/TiO_2 at X250, (c) Pt/Al_2O_3 at X250, and (d) Pt/AC at X1142.

with $C_i = 0$ at $t = 0$. The accumulation term, (dC_i/dt), is required especially when different start-up procedures are employed. The percentage conversion is calculated by

$$X_i(\%) = (R_{w,i} \cdot W)/(F_v^l \cdot C_{i,in}) \times 100\% \quad (2)$$

while the percentage selectivity (based on carbon atom) is calculated from equation (3) as

$$S_{\to j}(\%) = (n_{C,j} \cdot R_{w,j})/(n_{c,i} \cdot R_{w,i}) \times 100\% \quad (3)$$

Detailed data analysis procedures and other definitions used in this paper are described elsewhere [5]. For all experimental data, the overall carbon balance and the oxygen balance were verified after every experiment; they were within 95–100%, which was considered acceptable.

3. Results and discussion

3.1. Catalyst characterisation

The results of the particle size distribution and the BET analysis for platinum supported catalysts are shown in Table 1. It can be observed that the metal dispersion of Pt/TiO_2 (15.3%) is approximately three times as large as the metal dispersion of Pt/graphite (5.3%). The metal dispersion of Pt/Al_2O_3 and Pt/AC catalysts is 19.5% and 19.0%, respectively. Similar trend is observed for the metallic surface area per gram sample and per gram metal. Measurement of porosity of the catalyst support also shows comparable results, whereas Pt/AC is very porous (81.7%) as compared to other supports.

Figure 1 shows micrographs of platinum catalysts at different magnification, which were obtained from the SEM analysis. The graphite particles have irregular shapes and consist of layers (figure 1(a)). The size of graphite particles was estimated using the Coulter LS 130 apparatus. It can be see from figure 1(b) that TiO_2 particles have spherical shapes. It was also observed that the largest particles had a diameter of approximately 55 μm. figure 1(c) shows images of the platinum on alumina support in which the particles have similar spherical shapes. It was also observed that the largest particles had a diameter of approximately 160 μm. Similarly, Pt/AC particles have different physical shape as can be seen in (figure 1(d)). The micrographs clearly show that there are physical differences of the catalyst supports used in this study. The morphology of the support has an influence on the location of the active component, and therefore different exposure of the catalyst to the reactants is likely to affect the overall activity of the catalyst.

The location and distribution of the platinum metal depends normally on the methods and/or procedures employed during manufacturing of the catalysts. According to the manufacturers' information, Pt/graphite is an "eggshell" type whereby the platinum metals are distributed on the outer surface or edges of the pores. Other catalysts, namely: Pt/Al_2O_3, Pt/TiO_2, and Pt/AC are "mixed" type, i.e. platinum metals are located partly on surface/edges and deeper in pores. The effectiveness of these catalysts were examined in catalytic wet oxidation of model compounds namely, phenol, maleic acid, and malonic acid. The influences of such factors as the hydrophilic properties, and effects of the catalyst particle on mass transfer and reactor hydrodynamics were not the subject of this study.

3.2. Catalytic activity during phenol oxidation

The performances of the supported platinum catalysts were determined at temperatures of 135 and 165 °C and a total reactor pressure of 1.7 MPa, whereas the stoichiometric oxygen excess (S.E.) of 20% (mol/mol) was kept constant during phenol oxidation. The overall reaction for complete oxidation of phenol to CO_2 and H_2O is given by equation (4).

$$C_6H_5OH + 7O_2 \to 6CO_2 + 3H_2O \quad (4)$$

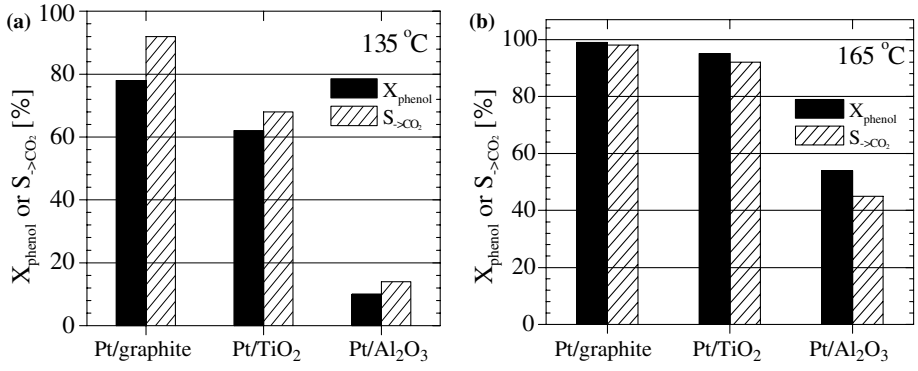


Figure 2. Disappearance of phenol and selectivity to CO_2 during phenol oxidation at standard condition (table 2) after 6.3 ks, over different supported Pt catalysts at S.E. = 20%: (a) conversion and selectivity to CO_2 at 135 °C, (b) conversion and selectivity to CO_2 at 165 °C.

The reaction proceeded rather slowly at 135 °C for all catalysts. Figure 2(a) shows the oxidation results for platinum on graphite, alumina and titanium oxide in terms of conversion and selectivity to CO_2 during phenol oxidation at 135 °C. Pt/graphite has a relatively high conversion of over 75% and selectivity to CO_2 of 92% at 135 °C, and liquid effluent samples changed from colourless to light yellow. The yellowish colour in the liquid sample possibly is due to the formation of *p*-benzoquinone and polymer precursors. The residual partial pressure of oxygen remained almost constant for about 2 h, thereafter a gradual increase was observed. About 62% conversion was attained after 1 h when Pt/TiO_2 was used and dropped gradually to reach 46% after 2 h, while the selectivity after 1 h was 65%. The residual oxygen partial pressure increased from 79 to 123 kPa. The performance of the Pt/Al_2O_3 catalyst is low at low temperature as can be seen from figure 2(a). A low conversion of less than 10% was observed at 135 °C. In addition, the effluent liquid was dark brownish in colour with suspended matter, probably polymeric products. The formation of *p*-benzoquinone indicates that few active sites are available for the catalytic reaction. Insoluble matter contribute to deactivation of the catalyst by fouling.

However, at high temperature, a significant change in the disappearance rate of phenol was observed. It can be seen in figure 2(b) that at 165 °C, high phenol conversion (>99%) and selectivity to CO_2 (98%) with Pt/graphite catalyst was obtained and the high activity of the catalyst was maintained. The effluent liquid was colourless without significant concentration of carboxylic acids or aromatic compounds (e.g. *p*-benzoquinone). Similar results were obtained with Pt/TiO_2 catalyst whereby phenol conversion above 95% and selectivity to CO_2 of ca. 92% was observed. Pt/Al_2O_3 catalyst gave poor performance with a conversion of 54% and selectivity to CO_2 less than 45%. The liquid effluent was characterised with the presence of a brownish colour with high concentration of *p*-benzoquinone. The formation of *p*-benzoquinone indicates over-oxidation of the active sites of the catalyst [5]. Deactivation of Pt/Al_2O_3 also has been explained by the formation of the less active form, PtO_2 [18,19].

The influence of a high oxygen load on the platinum catalyst performance was determined at 150 °C and a S.E. of 100%. Similar trends on the activity of the catalysts were observed as seen in figure 3. Pt/graphite catalyst shows relatively high activity and deactivation is rather slow or gradual. Once again low conversions and selectivity to CO_2 were observed for Pt/TiO_2 and Pt/Al_2O_3. After 8 ks the respective conversions were 93%, 31%, and 8% (figure 3a) for Pt/graphite, Pt/TiO_2, and Pt/Al_2O_3, whereas the selectivities (carbon basis) were 82%, 59%, and 7.5% (figure 3b), respectively. The corresponding residual oxygen partial pressures after 8 ks were 307, 524, and 572 kPa for Pt/graphite, Pt/TiO_2, and Pt/Al_2O_3, respectively. The effects of high residual oxygen partial pressures on the mechanisms of platinum on graphite catalysts and phenol oxidation pathways are reported elsewhere [15].

It can be concluded from figure 2 that an increase in temperature influences the activity of the platinum catalyst. At higher temperatures, the catalyst is able to handle higher oxygen and organic loads. While on the one hand poor performances are caused by high residual oxygen partial pressures, on the other hand the differences observed among the catalyst supports can be attributed to their differences in morphological and/or chemical properties. According to the manufacturer information, Pt/graphite is an "eggshell" catalyst with Pt metal located on the surface, while Pt/TiO_2, and Pt/Al_2O_3 are both "mixed" type with Pt metal partly on the edges and deeper in the pores. Since the experiments were performed at double the stoichiometric oxygen amount (S.E. of 100%) and sufficient degree of mixing (1200 rpm), several explanations are possible. The formation of polymer precursors is likely to cause deactivation for the inner active sites by fouling or blocking of pores for the "mixed" catalysts. From the results, it seems that the activity of the catalyst is related to the metal dispersion and porosity. Pt/graphite with a metal dispersion of 5.3% deactivates due to over-oxidation slowly compared to Pt/TiO_2, Pt/Al_2O_3 and

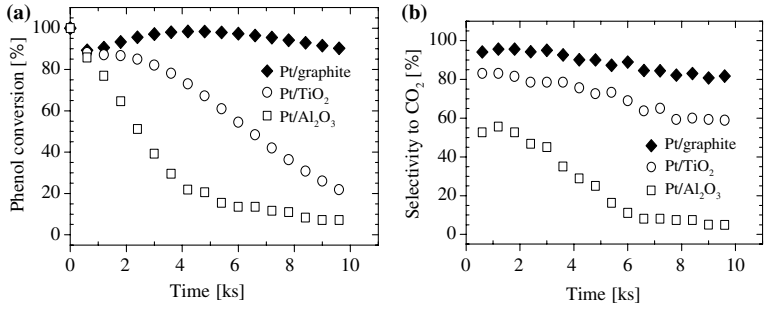


Figure 3. Phenol oxidation at standard conditions (table 2) over different supported Pt catalysts at 150 °C, and S.E. = 100%: (a) conversion and (b) selectivity to CO_2.

Table 2
Standard reactor operating conditions

Parameter	Standard	Range
Temperature (°C)	150	120–170
Total pressure (MPa)	1.7	1.5–1.8
Initial phenol concentration (mol/m^3)	20	20
Initial maleic acid concentration (mol/m^3)	20	20
Initial malonic acid concentration (mol/m^3)	20	20
Liquid flow rate (ml/min)	10	10
Oxygen flow rate (at room conditions) (ml/min)		
w.r.t. phenol flow rate	40.5	0–68
w.r.t. maleic acid flow rate	17.5	0–48
w.r.t. malonic acid flow rate	11.5	0–32
Nitrogen flow rate (at room conditions) (ml/min)	150	150
Liquid volume in the reactor (ml)	350	350
Catalyst (g)	3.5	0.5–7.0
Stirrer speed (rpm)	1200	350–1400
pH	Uncontrolled	2–7

Note: Standard oxygen flow rate is equivalent to S.E. of 20% with respect to the molar flow of organic compound.

Pt/AC with metal dispersions of 15.3%, 19.5%, and 19.0% respectively (table 1). Another possible explanation is that the support effect can be caused by platinum–support interaction, which may be larger for Pt/graphite due to electron transfer from the graphite to platinum particles. Gallezot *et al.* [10] reported that this electron transfer results in a different morphology and electronic structure of particles located on the edges of graphite layers than for particles located elsewhere. The differences in hydrophilic character of the catalyst cannot be overruled, since it has the potential to affect the affinity of the catalyst for the aqueous phase as well as the interaction between the support and the organic compound [11]. It is well known that Pt/graphite has low affinity for the aqueous phase.

3.3 Catalytic activity during maleic acid oxidation

The oxidation reaction of maleic acid to the desired end products CO_2 and H_2O is expressed by

$$COOH(CH)_2COOH + 3O_2 \rightarrow 4CO_2 + 2H2O \quad (5)$$

Comparative studies of catalyst supports were carried out at 150 °C and S.E. of 100% with catalysts concentration of 6.0 kg_{cat}/mL^3, while other reaction parameters were kept at standard conditions (table 2). Results show that Pt/graphite has the best performance in terms of maleic acid conversion and selectivity to CO_2 compared to Pt/Al_2O_3 and Pt/AC (see figure 4(a) and (b)). The trends shown for residual oxygen partial pressure (figure 4c) and residual maleic acid concentration (figure 4b) indicate the presence of deactivation. The observed deactivation of the catalyst is possibly due to the differences in properties of the supports. This is because all catalysts have the same loading of Pt metal of 5 wt%. A drop of conversion for Pt/graphite is clearly seen from 95% at after 1½ h to 81% after 3 h. The high pH of the liquid effluent (4.8), when Pt/graphite catalyst is used, indicates high conversion of maleic acid to CO_2 and H_2O. During the first 600 s, low

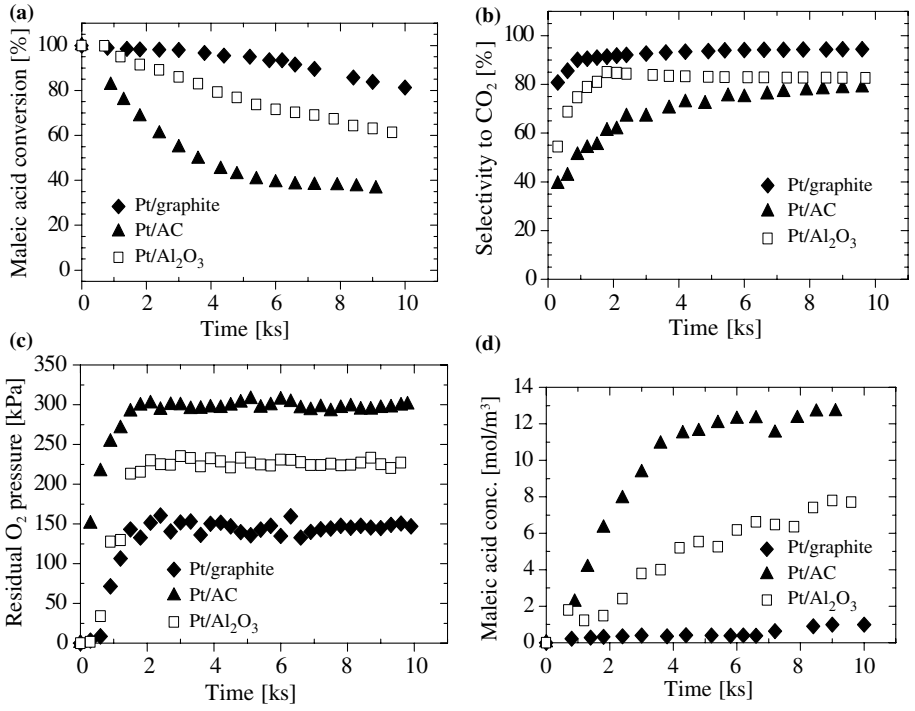


Figure 4. Maleic acid oxidation at standard conditions (table 2) over different supported Pt catalysts at 150 °C, S.E. = 100%, and 6 kg_{cat}/mL^3 catalyst: (a) conversion, (b) Selectivity to CO_2, (c) residual O_2 pressure and (d) concentration of maleic acid.

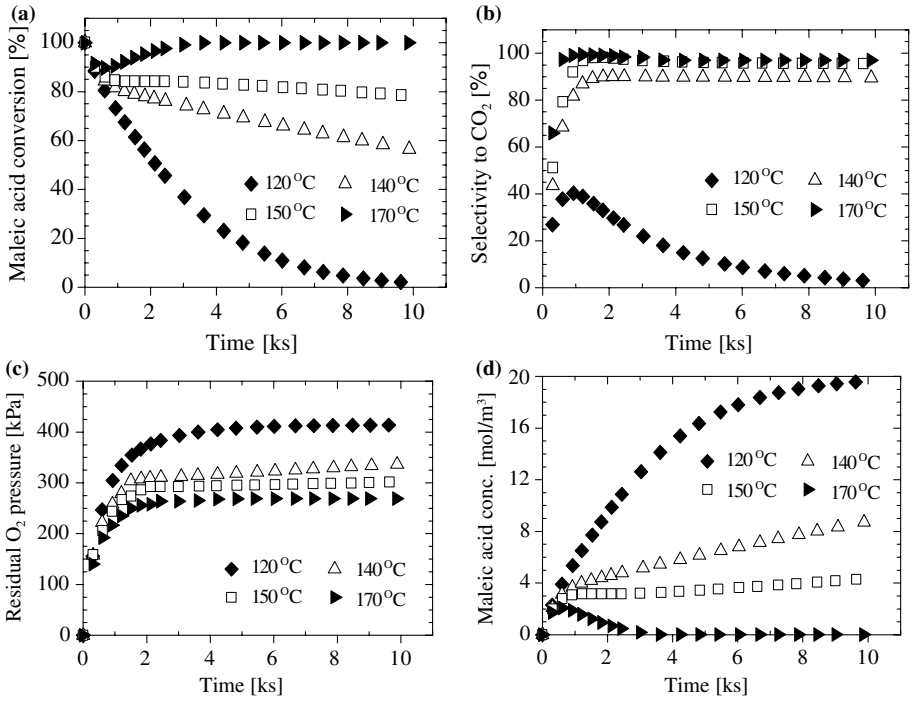


Figure 5. Effect of temperature during maleic acid oxidation using Pt/graphite at standard conditions (table 2) and S.E. = 200%: (a) conversion, (b) Selectivity to CO_2, (c) residual O_2 pressure and (d) concentration of maleic acid.

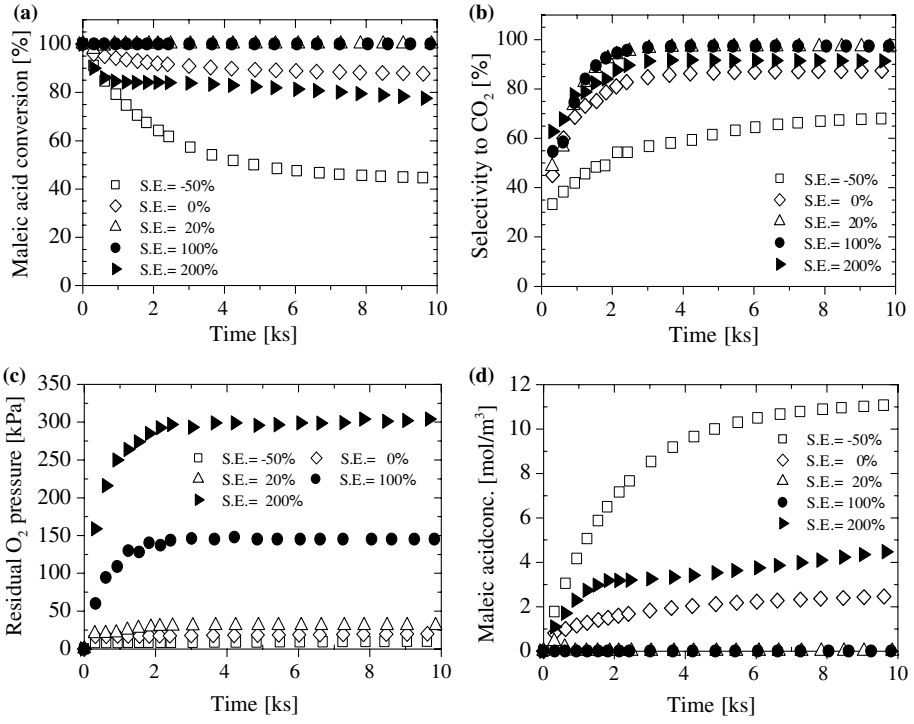


Figure 6. Effect of stoichiometric oxygen excess (S.E.) during maleic acid oxidation using Pt/graphite standard conditions and at 150 °C: (a) conversion, (b) Selectivity to CO_2, (c) residual O_2 pressure and (d) concentration of maleic acid.

concentrations of oxalic acid were detected which disappeared afterwards. The formation of oxalic acid at the start of the reaction was also observed when Pt/Al_2O_3 and Pt/AC were used. In all three catalysts, neither acetic acid nor succinic acid were observed in the liquid effluent. The formation of oxalic acid at the beginning of the reaction is attributed to the reactor start-up method [5] whereby oxygen concentration in

the liquid phase is initially low for the oxidation of maleic acid and oxalic acid. Furthermore, it can be inferred that oxidation of oxalic acid requires a partly oxidised platinum surface whereby the reaction to CO_2 proceeds via oxygen insertion [20]. The absence of acetic acid and succinic acid in the liquid effluent implies that these acids cannot be formed at high oxidation potential of the platinum catalyst; possibly they can be formed under oxygen-poor conditions.

The differences in activity observed between Pt/graphite and Pt/Al_2O_3 again can be attributed to differences in metal dispersion as previously explained. The differences in activity between Pt/graphite and Pt/AC are possibly due to the hydrophilic character of the support. Graphite is a more hydrophobic catalyst than activated carbon [11].

Pt/graphite was used to investigate the effects of temperature and oxygen partial pressure on the catalytic activity during maleic acid oxidation. The effect of temperature on the reaction rate was studied at a stoichiometric oxygen excess of 200% in the temperature range of 120–170 °C with a catalyst concentration of 10 kg_{cat}/mL^3 of Pt/graphite. It can be seen from figure 5(a) that the activity of the catalysts, which is expressed in terms of conversion, increases with temperature. Complete conversion of maleic acid to CO_2 and H_2O is achieved at 170 °C while at 120 °C low conversion and poor selectivity to CO_2 were obtained (see figure 5b). Figure 5(c) shows the residual oxygen partial pressure in the reactor while figure 5(d) shows a similar trend on the residual maleic acid concentration.

These observations indicate that a high temperature (>140 °C) enhances the reaction and the activity of the platinum catalyst. At high temperatures, the catalyst can handle higher oxygen and maleic acid loads. It was previously observed that when high oxygen loads are employed deactivation by over-oxidation takes place, however, at high temperature the activity of the catalyst was enhanced [5]. In order to discriminate the effects of temperature from that of oxygen loads, further experiments were performed at different oxygen concentration, expressed as S.E.

The influence of the oxygen molar flow rate (expressed as S.E.), during maleic acid oxidation was investigated at 150 °C at a catalyst concentration of 10 kg_{cat}/mL^3 of Pt/graphite. Other parameters were maintained at standard condition (table 2). It was found that the conversion of maleic acid increased with an increase in the oxygen molar flow with maximum conversion to CO_2 at S.E. of 20% figure 6(a). At high S.E. (100% and 200%) low carbon selectivity to CO_2 was obtained as seen in figure 6(b). The trend observed in figure 6(c) shows that the activity of the catalyst is decreased at very high residual oxygen partial pressure. In figure 6(d), the residual maleic acid concentration decreased with an increase in the oxygen flow for S.E. of −50%, 0%, 20%, and 100%, while a relatively high concentration was observed with S.E. of 200%.

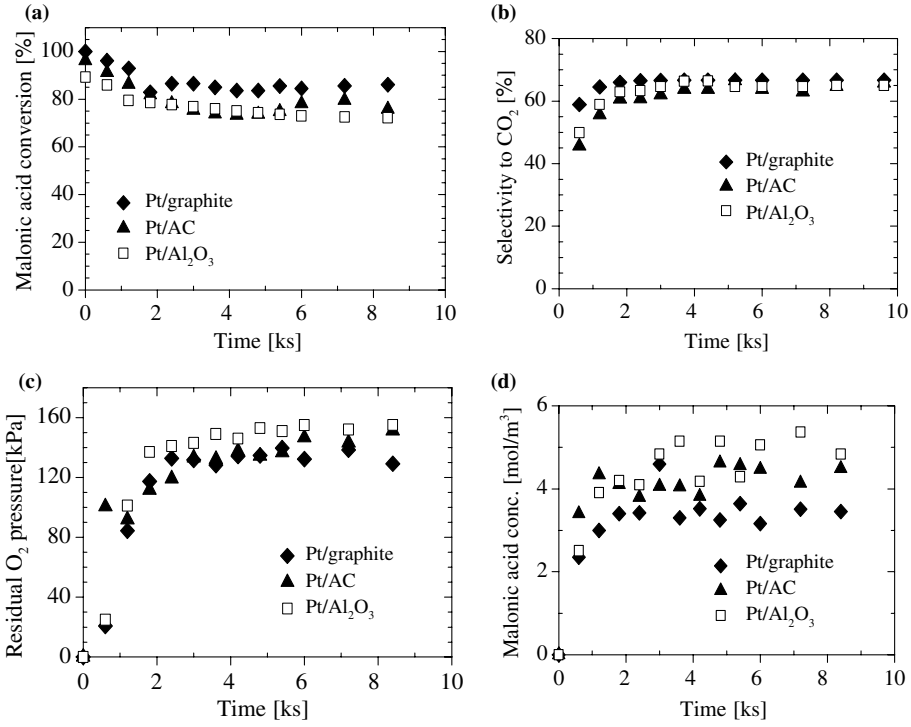


Figure 7. Malonic acid reaction at standard conditions (table 2) over supported Pt catalysts at 150 °C, and S.E. = 100%: (a) conversion, (b) selectivity to CO_2, (c) residual O_2 pressure and (d) malonic acid concentration.

The low activity of catalyst observed at high stoichiometric oxygen excess (e.g. S.E. of 200%) is possibly due to overoxidation of the catalyst active sites. It would have been expected that the highest CO_2 formation be at S.E. of 200% but it is lower than when S.E. of 0% and 100% are used. These results again support our previous observation during phenol oxidation that residual oxygen partial pressure, and hence too high oxygen load, is responsible for catalyst deactivation [5,15].

3.4. Catalytic activity during malonic acid oxidation

Figure 7 shows the performance of various catalysts during malonic acid oxidation at 150 °C and S.E. of 100%, while other parameters were kept at standard conditions (table 2). Malonic acid conversion was 85% for Pt/graphite whereas 74–78% were obtained for both Pt/Al_2O_3 and Pt/AC as shown in figure 7(a). It was further found that all catalysts gave comparable selectivity (carbon basis) to CO_2 within the range from 63% to 66% figure 7(b), while acetic acid was the only end products identified in liquid effluent. No other intermediates or end products were detected. Similar results were observed for residual oxygen partial pressures (figure 7(c)) and residual malonic acid concentration (figure 7(d)).

It can be inferred from these results that all catalysts have comparable performance under the test conditions. Since the residual oxygen partial pressure is high in all cases (about 150 kPa) and also the selectivity to CO_2 seems to be comparable (selectivity about 66%), it can be concluded that the oxidation of malonic acid is not the only route to CO_2. It indicates that the malonic acid reaction proceeds either through catalytic decarboxylation and oxidation or via non-catalytic decarboxylation. Homogeneous decarboxylation of malonic acid in the aqueous phase can be explained as

$$CH_2(COOH)_2 \rightarrow CO_2 + CH_3COOH \qquad (6)$$

In order to investigate whether malonic acid reaction proceeds via a catalytic or a non-catalytic route, a set of experiments was carried out at 150 °C with feed concentration of 20 mol/m^3. Figure 8 shows the results for malonic acid when the reaction is carried out under oxygen free environment (nitrogen only) without a catalyst present, with catalyst, and when both catalyst and oxygen are employed. High conversion rates for malonic acid were obtained when a catalyst was used as can be see in figure 8(a). During a blank experiment without oxygen (nitrogen only), about 0.88×10^{-6} mol/s of malonic acid degraded into CO_2 and acetic acid with molar selectivity of 100% each according to equation (6). However, the carbon selectivity to CO_2 was 33% after 2 h (figure 8(b)), whereas acetic acid was 67%. Furthermore, comparable disappearance rates for

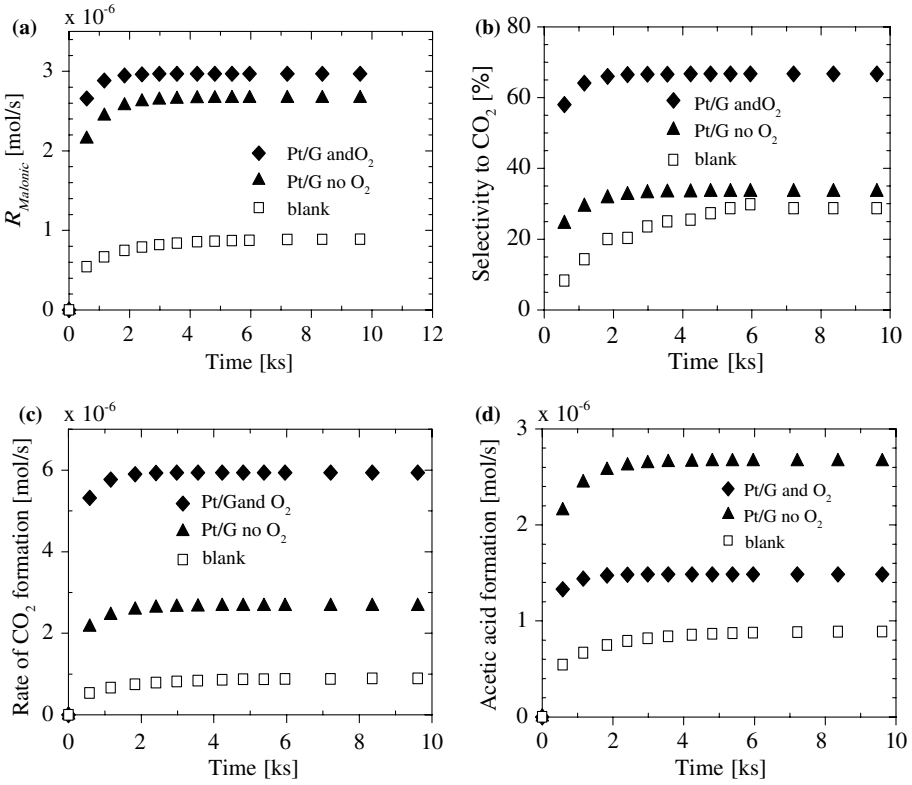


Figure 8. Catalysed and non-catalysed reaction of malonic acid at 150 °C, 1200 rpm, S.E. = 100%, $C_{malonic} = 20$ mol/m^3 and 10 kg_{cat}/mL^3 Pt/graphite: (a) reaction rate for malonic acid, (b) selectivity to CO_2, (c) acetic acid formation and (d) CO_2 formation.

malonic acid were observed during catalytic degradation without oxygen (2.66×10^{-6} mol/s) as well as with oxygen (2.97×10^{-6} mol/s). However, the carbon selectivity to CO_2 was different for catalytic degradation without oxygen (33%) as compared to catalytic oxidation (67%) of malonic acid. Similarly, a low rate of CO_2 formation was obtained during catalytic degradation without oxygen, which reached 2.7×10^{-6} mol/s after 2 h, whereas with oxygen a high rate is obtained (5.9×10^{-6} mol/s) as shown in figure 8(c). Significant differences were also observed on the rate of formation of acetic acid as shown in figure 8(d). While high rate for acetic acid formation was observed during catalytic reaction without oxygen (2.66×10^{-6} mol/s), about 1.49×10^{-6} mol/s acetic acid was attained when oxygen was added.

The results show that both homogeneous and catalytic decarboxylation give almost the same selectivity of the end products, CO_2 and acetic acid, however a high disappearance rate of malonic acid is achieved when the platinum catalyst is employed. It is further shown that when both catalyst and oxygen are used high selectivity to CO_2 is obtained, which confirms the presence of the oxidation route.

Another set of experiments was carried out at 150 °C with different oxygen molar flows (i.e. S.E. of 20% and 100%) to the reactor. It was found that in all cases, the disappearance rate of malonic acid remains relatively the same, i.e. from 5.9×10^{-6} to 6.0×10^{-6} mol/s. Furthermore, the maximum carbon selectivity to CO_2 was 68%, which is the same value as observed in figure 8(b). The results show that the influence of oxygen concentration on malonic acid conversion is very small whereas the selectivity to the end products CO_2 and H_2O is increased.

The influence of the temperature was also investigated to determine its effects on the conversion of malonic acid and selectivity to CO_2 and acetic acid. The investigation was carried out with 10 kg_{cat}/mL^3 of catalyst and in an oxygen-free environment (only nitrogen) to prevent oxidation. It is clearly seen in figure 9(a) that high temperature enhances the rate of disappearance of malonic acid. High disappearance rate of 3.2×10^{-6} mol/s for malonic acid (over 96% conversion) was achieved at 160 °C while 1.3×10^{-6} mol/s (about 40% conversion) was attained 120 °C. Within the range of temperatures studied, there is no significant difference in selectivity to CO_2, and the maximum achievable selectivity to CO_2 is 34% (figure 9(b)) and to acetic cid is 66%. Figure 9(c) also shows similar temperature dependence in terms of residual maleic acid. The rate of CO_2 formation also increases with temperature as can be seen in figure 9(d). The observed increase in conversion rate of malonic acid at high temperature during decarboxylation can be attributed to the increased catalytic activity of the platinum catalyst.

On the basis of the observed results, it is clear that malonic acid reaction proceeds via homogenous and

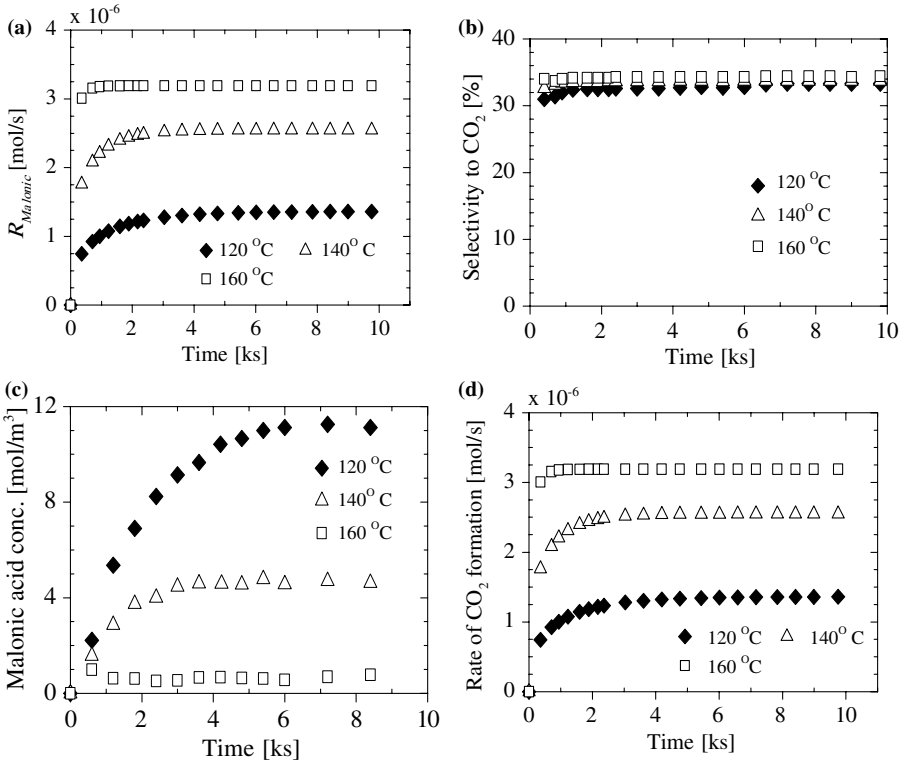


Figure 9. Effect of temperature during malonic acid reaction without oxygen at 1200 rpm, $C_{malonic} = 20$ mol/m^3 and 10 kg_{cat}/mL^3 Pt/graphite (a) reaction rate for malonic acid, (b) Selectivity to CO_2, (c) concentration of malonic acid and (d) CO_2 formation.

catalytic decarboxylation to CO_2 and acetic acid, and direct catalytic oxidation to CO_2 and H_2O. From figure 8 it appears that the homogeneous route for decarboxylation proceeds independently while the catalytic route leads to either decarboxylation and/or oxidation. Since the rate of CO_2 formation of 5.9×10^{-6} mol/s (figure 8(d)) during catalytic oxidation is twice the disappearance rate of malonic acid (2.9×10^{-6} mol/s), and the formation of acetic acid (1.5×10^{-6} mol/s) is almost half the disappearance of malonic acid, it seems that decarboxylation is not the only route. Although the catalytic mechanism for oxidation of malonic acid is not yet known, the catalytic routes can be expressed using the following equations:

$$\text{Decarboxylation} : CH_2(COOH)_2 \rightarrow CO_2 + CH_3COOH \quad (7)$$

$$\text{Oxidation} : CH_2(COOH)_2 + 2O_2 \rightarrow 3CO_2 + 2H_2O \quad (8)$$

When the catalytic reaction is carried out in the presence of oxygen, each of the reaction routes takes place, i.e. homogenous and catalytic decarboxylation, and oxidation. If we assume that malonic acid does not strongly adsorb on the catalyst, and the reactor wall and other impurities have no catalytic effects, the contribution of the individual reactions can be estimated based on the rates of formation of CO_2 (figure 8c) and acetic acid (figure 8(d)). It was found that, when both catalyst and oxygen are used, malonic acid reaction proceeds via homogenous decarboxylation, catalytic decarboxylation (equation (7)), and catalytic oxidation (equation (8)). The kinetics investigation of these reactions was not the subject of this study.

During catalytic reaction of malonic acid, acetic acid once formed was stable for the whole range of experimental conditions. It seems therefore, that oxidation of malonic acid involves decarboxylation, which forms an intermediate and H_{ads} (adsorbed H-atom) that can be oxidized. This surface intermediate is possibly–CH_2–COOH, whereby a highly oxidised platinum surface takes the H-atom (H_{ads}) before it can recombine to form acetic acid. In absence of oxygen, the catalyst surface is in a reduced state, which means that after decarboxylation the intermediates can recombine with H-atoms, thus favouring acetic acid formation. The role of oxygen during catalytic oxidation is therefore to enhance the selectivity to the desired end products CO_2 and H_2O as well as to impair the formation of acetic acid.

4. Conclusions

This work shows that the catalyst support type and the platinum dispersion have a significant effect on the reaction rate during CWO of organic wastes. Pt/graphite catalyst was found to be most effective and stable throughout the range of experimental conditions used. Pt/graphite, which has a metal dispersion of 5.3%, deactivates (over-oxidation) slowly compared to Pt/TiO_2 (15.3%), Pt/Al_2O_3 (19.5%) and Pt/AC (19.0%). Deactivation by fouling or blocking of active sites is one of the consequences of over-oxidation, particularly during phenol oxidation whereby *p*-benzoquinone and polymer precursors are formed. Deactivation by fouling seems to be severe for "mixed" type catalysts, e.g. Pt/Ti_2O_2, Pt/Al_2O_3, and Pt/AC, which also have relatively high metal dispersion and high porosity as compared to Pt/graphite catalyst.

During oxidation of maleic acid at 150 °C with a catalyst concentration of 6.0 kg_{cat}/mL^3, Pt/graphite again was found to be effective followed by Pt/Al_2O_3 and Pt/AC. Furthermore, complete conversion of maleic acid to CO_2 and H_2O was achieved at 150 °C and S.E. of 100% when 10 kg_{cat}/mL^3 of Pt/graphite was used. At high temperatures, the activity of the Pt/graphite is enhanced, and complete conversion can be obtained even with high oxygen loads.

Despite the differences of the morphological properties of the catalysts, the activity of the investigated support materials for platinum catalysts decreases in the order Pt/graphite > Pt/TiO_2 > Pt/Al_2O_3, as observed during phenol oxidation, and Pt/graphite > Pt/Al_2O_3 > Pt/AC during maleic acid oxidation. It seems that the metal dispersion is one of the explanations for the differences in activity of the catalysts. The effect of platinum–support interaction however, cannot be excluded, which may be larger for Pt/graphite due to electron transfer from the graphite support to the platinum particle. Furthermore, differences in catalytic activity between Pt/graphite and Pt/Active carbon also can be attributed to the difference in hydrophilic character of the catalyst, where Pt/graphite has the lowest affinity for the aqueous phase.

The reaction of malonic acid in the presence of Pt/graphite catalyst and oxygen proceeds via homogeneous or non-catalysed decarboxylation, and catalytic decarboxylation to CO_2 and acetic acid, and catalytic oxidation to CO_2 and H_2O. The oxidation of malonic acid involves decarboxylation that gives intermediates, which can be oxidized at a highly oxidised platinum surface before desorption as acetic acid takes place. Without oxygen the catalyst surface is in a reduced state and this favours the intermediates to recombine with H_{ads} to form acetic acid. Acetic acid, which was formed during catalytic decarboxylation, is a refractory compound that was difficulty to oxidize at the conditions tested.

Acknowledgments

The funding for this research was provided by the Dutch Government (NUFFIC) through the EVEN project (MHO/UDSM/EUT/EVEN). The technical

assistance of M.E. Coolen-Kuppens and W. Kazimbaya is gratefully acknowledged. Thanks are due to T.L.M. Vorage and E. Mwakibolwa for their participation in this project.

References

[1] Yu.I. Matatov-Meytal and M. Sheintuch, Ind. Eng. Chem. Res. 37 (1998) 309.
[2] V.S. Mishra, V.V. Mahajani and J.B. Joshi, Ind. Eng. Chem. Res. 34 (1995) 2.
[3] F. Luck, Catal. Today 53 (1999) 81.
[4] J. Levec and A. Pintar, Catal. Today 24 (1995) 51.
[5] Z.P.G. Masende, B.F.M. Kuster, K.J. Ptasinski, F.J.J.G. Janssen, J.H.Y. Katima and J.C. Schouten, Appl. Catal. B 41 (2003a) 247.
[6] J.C. Beziat, M. Besson, P. Gallezot and S. Durecu, Ind. Eng. Chem. Res. 38 (1999) 1310.
[7] L. Oliviero, Jr. J. Barbier, D. Duprez, A. Guerrero-Ruiz, B. Bachiller-Baeza and I. Rodriguez-Ramos, Appl. Catal. B 25(4) (2000) 267.
[8] P. Gallezot, S. Chaumet, A. Perrard and P. Insard, J. Catal. 168(1) (1997) 104.
[9] A. Fortuny, J. Font and A Fabregat, Appl. Catal. B 19(3–4) (1998) 165.
[10] P. Gallezot, D. Richard and G. Bergeret, in Novel Materials in Heterogeneous Catalysis eds. R.T.K. Baker and L.L. Murrel, *ACS Symposium Series*, Vol. 437, (ACS, Washington, DC, 1990) p. 150.
[11] J.H. Vleeming, *Deactivation of carbon-supported platinum catalysts during carbohydrate oxidation*, *Ph.D. thesis* (Eindhoven University of Technology, Eindhoven, 1997).
[12] C. Perego and S. Peratello, Catal. Today 52 (1999) 133.
[13] G. Donati and R. Paludetto, Catal. Today 52 (1999) 183.
[14] H.S. Fogler, *Elements of Chemical Reaction Engineering*, 3rd edn. (Prentice Hall, Upper Saddle River NJ, 1999), p. 577.
[15] Z.P.G. Masende, B.F.M. Kuster, K.J. Ptasinski, F.J.J.G. Janssen, J.H.Y. Katima and J.C. Schouten, Catal. Today 79–80 (2003b) 357.
[16] J.J.F. Scholten, in: *Catalysis, An Integrated Approach to Homogeneous, Heterogeneous and Industrial Catalysis* eds. J.A. Moulijn, P.W.M.N. Van Leeuwen and Van Santen, *Studies in Surface Science and Catalysis*, Vol. 79, (Elsevier, Amsterdam, 1993). p. 419.
[17] G. Charlot, *Les méthodes de la chimie analytique*, (Mason, Paris 1961) p. 859.
[18] J.E. Bauer, M.L. Occelli, P.M. Williams and P.C. McCaslin, and Marine Chemistry, 41 (1993) 75–89.
[19] J.J. Ostermaier, J.R. Katzer and W.H. Manogue, J. Catal. 41 (1976) 277.
[20] A.P. Markusse, B.F.M. Kuster and J.C. Schouten, Stud. Surf. Sci. Catal. 126 (1999) 273.